

# Synthesis of a Tetracopper Assembly Complex Comprised of One Macrocyclic Dinuclear Copper Unit and Two Mononuclear Copper Units: Intramolecular Electron Transfer Relevant to Multicopper Oxidase

Yuko Suetsugu, Yuko Mitsuka, Yuji Miyasato, Masaaki Ohba,<sup>†</sup> and Hisashi Ōkawa\*

Department of Chemistry, Faculty of Science, Kyushu University, 6-10-1 Hakozaki, Higashi-ku, Fukuoka 812-8581

Received July 7, 2005; E-mail: okawascc@mbox.nc.kyushu-u.ac.jp

The dinuclear copper(II) complex  $[\text{Cu}_2(\text{L}^1)](\text{ClO}_4)_2 \cdot \text{CH}_3\text{OH} \cdot 2\text{H}_2\text{O}$  (**1**) of a macrocyclic ligand  $\text{H}_2\text{L}^1$ , derived from the cyclic [2:2] condensation of 2,6-diformyl-4-methylphenol and 1,1,1-tri(aminomethyl)ethane, has been prepared as the type 3 copper site for modeling multicopper oxidase: **1** has two auxiliary amino groups on the macrocyclic framework. The condensation of **1** with two molecules of 2-formylpyridine through the amino groups afforded  $[\text{Cu}_2(\text{L}^2)](\text{ClO}_4)_2 \cdot 2\text{DMF}$  (**2**). This has a Cu...Cu separation of 4.434(1) Å with no direct bridge between the two copper atoms, owing to the involvement of the auxiliary 2-pyridylmethylimino residue in coordination. The condensation of **1** with two molecules of 3-[*N,N*-di(2-pyridylmethyl)aminomethyl]-5-methylsalicylaldehyde in the presence of  $\text{Cu}(\text{ClO}_4)_2 \cdot 6\text{H}_2\text{O}$  afforded the tetracopper assembly complex  $[\text{Cu}_4(\text{L}^3)](\text{ClO}_4)_4 \cdot 3\text{H}_2\text{O}$  (**3**), which is comprised of a macrocyclic dinuclear  $\text{Cu}_2(\text{II},\text{II})$  unit and two mononuclear Cu(II) units,  $\{\text{Cu}(\text{II})-\text{Cu}_2(\text{II},\text{II})-\text{Cu}(\text{II})\}$ . Cyclic voltammograms of **3** exhibit a two-electron redox process at  $-0.77$  V (vs  $\text{Ag}/\text{Ag}^+$ ) followed by two one-electron redox processes at  $-0.85$  and  $-1.29$  V. Coulometric studies combined with spectroscopic and EPR studies demonstrate that the redox process at  $-0.77$  V involves the reduction of two mononuclear Cu(II) units followed by an intramolecular electron transfer from one of the reduced Cu(I) units to the dinuclear  $\text{Cu}_2(\text{II},\text{II})$  unit:  $\{\text{Cu}(\text{II})-\text{Cu}_2(\text{II},\text{II})-\text{Cu}(\text{II})\} \rightarrow \{\text{Cu}(\text{I})-\text{Cu}_2(\text{II},\text{II})-\text{Cu}(\text{I})\} \rightarrow \{\text{Cu}(\text{I})-\text{Cu}_2(\text{I},\text{II})-\text{Cu}(\text{II})\}$ . The resulting  $\{\text{Cu}(\text{I})-\text{Cu}_2(\text{I},\text{II})-\text{Cu}(\text{II})\}$  species is further reduced to  $\{\text{Cu}(\text{I})-\text{Cu}_2(\text{I},\text{I})-\text{Cu}(\text{I})\}$  at  $-0.85$  V and to  $\{\text{Cu}(\text{I})-\text{Cu}_2(\text{I},\text{I})-\text{Cu}(\text{I})\}$  at  $-1.29$  V.

Multicopper oxidases such as laccase and ascorbate oxidase have all three types of copper (monometallic type 1, monometallic type 2, and dimetallic type 3) at the active site and catalyze the four-electron reduction of dioxygen to water with concomitant oxidation of a substrate.<sup>1,2</sup> The simplest of this family is laccase, which contains four copper atoms from each of three types of copper.<sup>3</sup> Ascorbate oxidase has two subunits and each subunit has a marked resemblance to that of laccase.<sup>4</sup> X-ray crystallographic studies for the oxidized form of ascorbate oxidase from zucchini squash have revealed a triangular cluster formed by type 2 copper and type 3 copper; the type 1 copper is separated by ca. 12 Å from the type 3 copper.<sup>5</sup> A similar constellation of three types of copper is confirmed for ceruloplasmin.<sup>6</sup> Based on studies of laccase derivatives, the triangular cluster was shown to be the minimum unit for dioxygen reduction.<sup>7</sup> Thus, initial model studies on multicopper oxidases were devoted to replicating the triangular copper cluster.<sup>8–10</sup> However, the involvement of type 1 copper in biological function is obvious: type 1 copper receives an electron from the substrate and transfers the electron, in conjunction with type 2 copper, to type 3 center which is the site of dioxygen interaction.<sup>11</sup> Because of this reason, our attention in modeling multicopper oxidase is denoted to tetracopper assembly

complexes comprised of a dinuclear copper unit as type 3 copper and two auxiliary mononuclear copper units as type 1 copper and type 2 copper.<sup>12,13</sup>

The most essential in modeling multicopper oxidase is the design of type 3 copper site; the dinuclear  $\text{Cu}_2(\text{II},\text{II})$  unit must be stable in redox process and have a high reduction potential so as to be reduced to  $\text{Cu}_2(\text{I},\text{II})$  and to  $\text{Cu}_2(\text{I},\text{I})$ . The di( $\mu$ -phenolato) dinuclear copper(II) complex of the macrocyclic ligand  $\text{H}_2\text{L}$  (Fig. 1, left) can be a good candidate for type 3 copper site since the dinuclear  $\text{Cu}_2(\text{II},\text{II})$  core is stabilized by the macrocyclic effect<sup>14</sup> of the ligand and is reduced to  $\text{Cu}_2(\text{I},\text{II})$  and then to  $\text{Cu}_2(\text{I},\text{I})$  species in available potential.<sup>15–17</sup> In this work, we have prepared the dinuclear copper(II) complex  $[\text{Cu}_2(\text{L}^1)]$ -

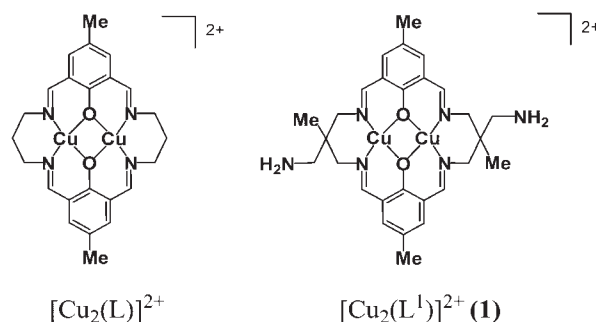
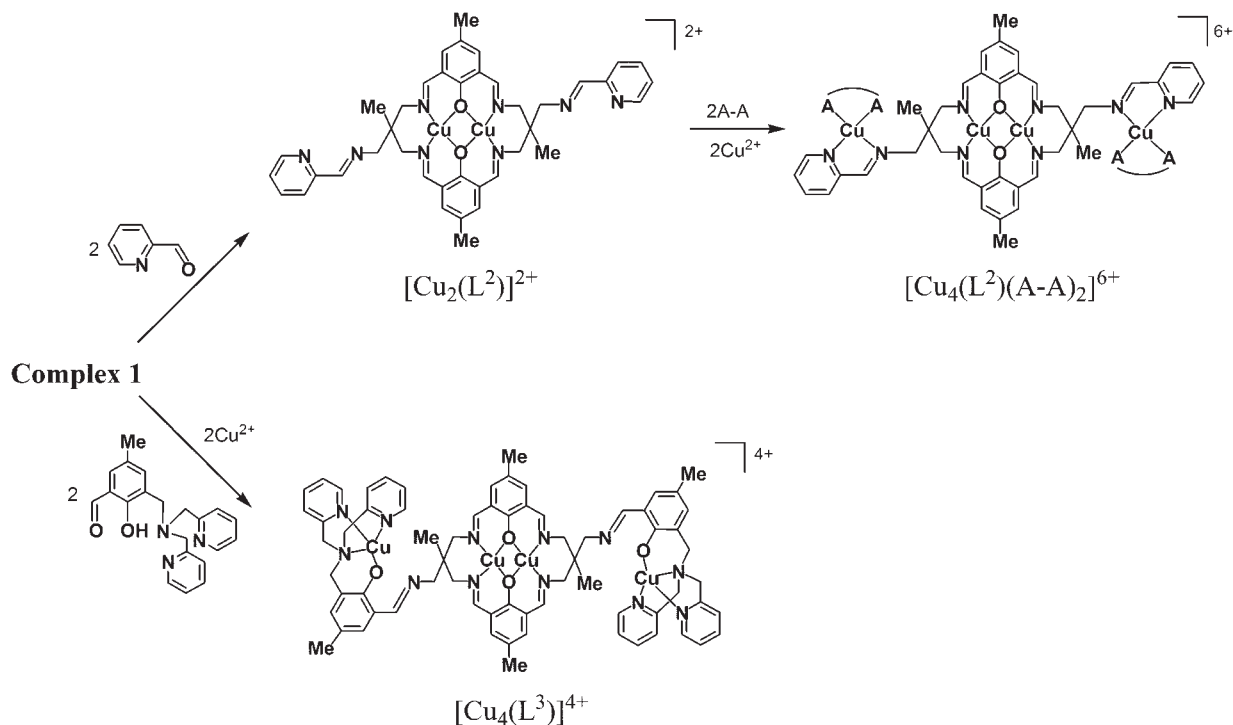


Fig. 1. Chemical structures of  $[\text{Cu}_2(\text{L})]^{2+}$  (left) and  $[\text{Cu}_2(\text{L}^1)](\text{ClO}_4)_2 \cdot \text{CH}_3\text{OH} \cdot 2\text{H}_2\text{O}$  (**1**) (right).

<sup>†</sup> Present address: Graduate School of Engineering, Department of Synthetic Chemistry and Biological Chemistry, Kyoto University, Katsura, Nishikyo-ku, Kyoto 615-8510

Fig. 2. Strategies for producing tetracopper assembly complexes from **1**.

$(\text{ClO}_4)_2 \cdot \text{CH}_3\text{OH} \cdot 2\text{H}_2\text{O}$  (**1**) of analogous ligand  $\text{H}_2\text{L}^1$  (Fig. 1, right) that has two auxiliary amino groups available as connectors for introducing two mononuclear copper units. Our strategies for introducing two mononuclear copper units into **1** are shown in Fig. 2. In one approach, **1** is condensed with two molecules of 2-formylpyridine through the auxiliary amino groups to obtain  $[\text{Cu}_2(\text{L}^2)]^{2+}$ , which can be a good precursor of tetracopper assembly complexes  $[\text{Cu}_4(\text{L}^2)(\text{A-A})_2]^{6+}$  (A-A: bidentate chelating ligand). In another approach, **1** is condensed with two molecules of 3-[N,N-di(2-pyridylmethyl)amino-methyl]-5-methylsalicylaldehyde in the presence of  $\text{Cu}(\text{ClO}_4)_2 \cdot 6\text{H}_2\text{O}$ , with a hope to obtain a tetracopper assembly complex  $[\text{Cu}_4(\text{L}^3)]^{4+}$ . We report the synthesis of **1**,  $[\text{Cu}_2(\text{L}^2)](\text{ClO}_4)_2 \cdot 2\text{DMF}$  (**2**) and  $[\text{Cu}_4(\text{L}^3)](\text{ClO}_4)_4 \cdot 3\text{H}_2\text{O}$  (**3**) and an intramolecular electron transfer in **3** relevant to multicopper oxidase.

### Experimental

**Preparation.** 2,6-Diformyl-4-methylphenol,<sup>18</sup> 1,1,1-tri(aminomethyl)ethane trihydrochloride,<sup>19,20</sup> and 3-[N,N-di(2-pyridylmethyl)aminomethyl]-5-methylsalicylaldehyde<sup>21</sup> were prepared by the literature methods. Other chemicals were purchased from commercial sources and used without further purification.

**$[\text{Cu}_2(\text{L}^1)](\text{ClO}_4)_2 \cdot \text{CH}_3\text{OH} \cdot 2\text{H}_2\text{O}$  (**1**).** 2,6-Diformyl-4-methylphenol (166 mg, 1.0 mmol) and copper(II) perchlorate hexahydrate (404 mg, 1.1 mmol) were dissolved in methanol (15  $\text{cm}^3$ ). To this was added a solution of 1,1,1-tri(aminomethyl)ethane trihydrochloride (263 mg, 1.0 mmol) and triethylamine (340 mg) in methanol (5  $\text{cm}^3$ ), and the mixture was stirred at the boiling temperature for 3 h. The resulting green solution was condensed to ca. 5  $\text{cm}^3$  and diffused with ether to obtain a green powder. It was dissolved in methanol and the solution was diffused with 2-propanol to give green microcrystals. The yield was 335 mg (38%). Anal. Found: C, 39.27; H, 5.27; N, 9.41; Cu, 14.13%. Calcd

for  $[\text{Cu}_2(\text{L}^1)](\text{ClO}_4)_2 \cdot \text{CH}_3\text{OH} \cdot 2\text{H}_2\text{O}$  ( $\text{C}_{29}\text{Cl}_2\text{Cu}_2\text{H}_{44}\text{N}_6\text{O}_{13}$ ): C, 39.46; H, 5.02; N, 9.52; Cu, 14.40%. Selected IR [ $\nu/\text{cm}^{-1}$ ] using KBr: 3400–3200, 1637, 1110, 1089, 626.  $\mu_{\text{eff}}$  per molecule: 1.57  $\mu_{\text{B}}$  (at 298 K)–0.57  $\mu_{\text{B}}$  (at 2 K). UV–vis data [ $\lambda/\text{nm}$  ( $\epsilon/\text{dm}^3 \text{mol}^{-1} \text{cm}^{-1}$ )] in DMF: 362 (11000),  $\approx$ 385 (shoulder), 640 (165).

**$[\text{Cu}_2(\text{L}^2)](\text{ClO}_4)_2 \cdot 2\text{DMF}$  (**2**).** A solution of 2-formylpyridine (109 mg, 1.0 mmol) in methanol (10  $\text{cm}^3$ ) was dropwise added to a stirred solution of **1** (440 mg, 0.5 mmol) in methanol (5  $\text{cm}^3$ ) to obtain a green precipitate. It was dissolved in DMF (30  $\text{cm}^3$ ) and the solution was diffused with 2-propanol to obtain green needles. This was proved to be  $[\text{Cu}_2(\text{L}^2)](\text{ClO}_4)_2 \cdot 2\text{DMF}$  based on X-ray crystallography as discussed later. The yield was 200 mg (40%). The crystals were efflorescent in open air. Elemental analyses obtained for a sample dried in vacuo agreed with  $[\text{Cu}_2(\text{L}^2)](\text{ClO}_4)_2$ . Anal. Found: C, 48.06; H, 4.28; N, 11.20; Cu, 12.80%. Calcd for  $[\text{Cu}_2(\text{L}^2)](\text{ClO}_4)_2$  ( $\text{C}_{40}\text{Cl}_2\text{Cu}_2\text{H}_{42}\text{N}_8\text{O}_{10}$ ): C, 48.39; H, 4.26; N, 11.29; Cu, 12.80%. Selected IR [ $\nu/\text{cm}^{-1}$ ] using KBr: 1636, 1088, 625.  $\mu_{\text{eff}}$  per copper: 1.84  $\mu_{\text{B}}$  at 298 K. UV–vis data [ $\lambda/\text{nm}$  ( $\epsilon/\text{dm}^3 \text{mol}^{-1} \text{cm}^{-1}$ )] in DMF: 362 (11000),  $\approx$ 385 (shoulder), 620 (165).

**$[\text{Cu}_4(\text{L}^3)](\text{ClO}_4)_4 \cdot 3\text{H}_2\text{O}$  (**3**).** A solution of 3-[N,N-di(2-pyridylmethyl)aminomethyl]-5-methylsalicylaldehyde (354 mg, 1.0 mmol) in methanol (10  $\text{cm}^3$ ) was dropwise added to a solution of **1** (440 mg, 0.5 mmol) in methanol (5  $\text{cm}^3$ ), and the mixture was stirred at the reflux temperature for 30 min. To the resulting deep green solution was added a solution of copper(II) perchlorate hexahydrate (374 mg, 1.0 mmol) in methanol (5  $\text{cm}^3$ ) to afford a green precipitate. It was dissolved in pyridine and the solution was diffused with 2-propanol to give green microcrystals. The yield was 940 mg (51%). Anal. Found: C, 45.38; H, 4.23; N, 9.22; Cu, 13.78%. Calcd for  $[\text{Cu}_4(\text{L}^3)](\text{ClO}_4)_4 \cdot 3\text{H}_2\text{O}$  ( $\text{C}_{70}\text{Cl}_4\text{Cu}_4\text{H}_{78}\text{N}_{12}\text{O}_{23}$ ): C, 45.41; H, 4.25; N, 9.08; Cu, 13.73%. Selected IR [ $\nu/\text{cm}^{-1}$ ] using KBr: 1638, 1093, 624.  $\mu_{\text{eff}}$  per molecule: 3.15  $\mu_{\text{B}}$  (at 298 K)–2.74  $\mu_{\text{B}}$  (at 2 K). UV–vis data [ $\lambda/\text{nm}$  ( $\epsilon/\text{dm}^3 \text{mol}^{-1} \text{cm}^{-1}$ )] in DMF: 362 (11000),  $\approx$ 385 (shoulder), 620 (165).

$\text{dm}^3 \text{mol}^{-1} \text{cm}^{-1}$ ] in DMF: 360 (15200),  $\approx 380$  (ca. 10000), 420 (ca. 6000), 665 (290). Positive ESI mass in the presence of tetra-(*n*-butyl)ammonium chloride:  $m/z = 1506$  for  $\{\text{Cu}_4(\text{L}^3)\text{Cl}_3\}^+$ .

**Physical Measurements.** Elemental analyses of carbon, hydrogen, and nitrogen were obtained at The Service Center of Elemental Analysis of Kyushu University. Analyses of copper were obtained using a Shimadzu AA-680 Atomic Absorption/Flame Emission Spectrophotometer. Infrared spectra were measured using KBr disk on a Perkin-Elmer Spectrum BX FT-IR system. Electronic absorption spectra in DMF were recorded on a Shimadzu UV-3100PC spectrophotometer. Magnetic susceptibilities of powdered samples were measured on a Quantum Design MPMS XL SQUID susceptometer. X-band electron paramagnetic resonance (EPR) spectra were recorded on a JES-FE3X spectrometer. Cyclic voltammograms were recorded using a BAS CV-50W electrochemical analyzer in DMF solution containing tetra(*n*-butyl)ammonium perchlorate (TBAP) as the supporting electrolyte (**Caution!** TBAP is explosive and should be handled with great care). A three-electrode cell was used that was equipped with a glassy carbon working electrode, a platinum coil as the counter electrode, and a AgCl/Ag (TBAP/acetonitrile) electrode as the reference. Coulometric studies were carried out on the same apparatus using a platinum net as the working electrode.

**X-ray Crystallography.** A single crystal of **2** was mounted on a glass fiber and coated by epoxy resin. Crystallographic measurements were carried out on a Rigaku/MSM Mercury diffractometer at  $-90^\circ\text{C}$  with graphite monochromated Mo  $K\alpha$  radiation ( $\lambda = 0.71070 \text{ \AA}$ ). A symmetry-related absorption correction using the program ABSCOR and an empirical absorption correction based on azimuthal scans of several reflections were applied. Crystallographic parameters are summarized in Table 1.

The structure was solved by the direct method and expanded using Fourier technique. Non-hydrogen atoms were refined anisotropically. Hydrogen atoms were included in the structure analysis but not refined. All calculations were performed using the teXsan crystallographic software package of Molecular Structure Corporation.<sup>22</sup>

Table 1. Crystallographic Parameters for  $[\text{Cu}_2(\text{L}^2)](\text{ClO}_4)_2 \cdot 2\text{DMF}$  (**2**)

Formula	$\text{C}_{46}\text{H}_{56}\text{N}_{10}\text{Cl}_2\text{Cu}_2\text{O}_{12}$
Formula weight	1139.02
Color	green
Crystal system	triclinic
Space group	$P\bar{1}$ (No. 2)
$a/\text{\AA}$	7.2133(7)
$b/\text{\AA}$	11.639(1)
$c/\text{\AA}$	14.368(1)
$\alpha/^\circ$	91.832(6)
$\beta/^\circ$	92.226(7)
$\gamma/^\circ$	95.218(7)
$V/\text{\AA}^3$	1199.6(1)
Z value	1
$D_{\text{calcd}}/\text{g cm}^{-3}$	1.576
$\mu(\text{Mo } K\alpha)/\text{cm}^{-1}$	10.72
No. observations	5387
$R$ (all data)	0.067
$R_1$ ( $>2.0\sigma(I)$ )	0.046
$R_w$	0.142
G.O.F.	1.00

Crystallographic data have been deposited at the Cambridge Crystallographic Data Centre as supplementary publication No. CCDC-264282. Copies of the data can be obtained free of charge via <http://www.ccdc.cam.ac.uk/conts/retrieving.html> (or from the Cambridge Crystallographic Data Centre, 12, Union Road, Cambridge, CB2 1EZ, UK; Fax: +44 1223 336033; E-mail: deposit@ccdc.cam.ac.uk).

## Results and Discussion

**Synthesis and General Characterization.** Complex **1** was prepared by the cyclic [2:2] condensation of 2,6-diformyl-4-methylphenol and 1,1,1-tri(aminomethyl)ethane in the presence of  $\text{Cu}(\text{ClO}_4)_2 \cdot 6\text{H}_2\text{O}$  in methanol. The magnetic moment of **1** is  $1.57 \mu_{\text{B}}$  per molecule ( $1.11 \mu_{\text{B}}$  per Cu) at room temperature, and the moment decreased with lowering temperature to  $0.57 \mu_{\text{B}}$  per molecule ( $0.40 \mu_{\text{B}}$  per Cu) at 2 K (Fig. 3). Such magnetic behavior is often observed for di( $\mu$ -phenolato) dicopper(II) complexes<sup>23,24</sup> and explained by antiferromagnetic interaction through the phenolic oxygen bridges. The non-zero magnetic moment at low temperature suggests contamination of paramagnetic impurity. Thus, magnetic simulations were carried out by the modified Bleaney–Bowers equation,<sup>25</sup>

$$\chi_A = (1 - \rho)\{Ng^2\beta^2/kT\} \times [3 + \exp(-2J/kT)]^{-1} + \rho \times \{Ng^2\beta^2/4kT\} + N\alpha, \quad (1)$$

where  $\rho$  is the fraction of paramagnetic impurity and other symbols have their usual meanings. The magnetic property of **1** can be explained by this equation using  $g = 2.07$ ,  $J = -270 \text{ cm}^{-1}$ ,  $N\alpha = 80 \times 10^{-6} \text{ cm}^3 \text{mol}^{-1}$ , and  $\rho = 0.05$ , as in-

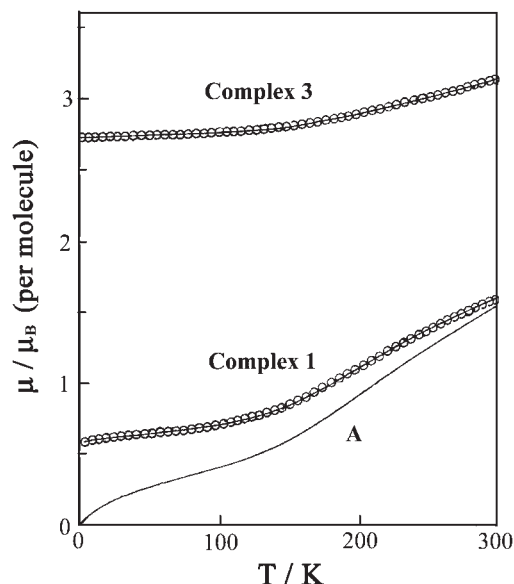


Fig. 3. Temperature-dependence of magnetic moment (per molecule) of  $[\text{Cu}_2(\text{L}^1)](\text{ClO}_4)_2 \cdot \text{CH}_3\text{OH} \cdot 2\text{H}_2\text{O}$  (**1**) and  $[\text{Cu}_4(\text{L}^3)](\text{ClO}_4)_4 \cdot 3\text{H}_2\text{O}$  (**3**). The magnetism of **1** is explained by the modified Bleaney–Bowers equation using  $g = 2.07$ ,  $J = -270 \text{ cm}^{-1}$ ,  $N\alpha = 80 \times 10^{-6} \text{ cm}^3 \text{mol}^{-1}$ , and  $\rho = 0.05$ . Trace A is the  $\mu$  vs  $T$  curve for **1** in the absence of paramagnetic impurity ( $\rho = 0$ ). The magnetism of **3** is explained by the equation,  $\mu^2 = \mu_{\text{CuCu}}^2 + 2\mu_{\text{Cu}}^2$ , using  $1.93 \mu_{\text{B}}$  for the mononuclear unit and trace A for the dinuclear unit.

licated by the solid line. The  $\mu$  vs  $T$  curve for **1** in the absence of the paramagnetic impurity is shown by trace **A**; this curve is used later for the magnetic analysis of the tetracopper assembly complex **3**.

Complex **1** seems not to be sensitive toward atmospheric carbon dioxide. Furthermore, the d–d band maximum of **1** (640 nm) is located at a longer wavelength relative to that of its parent complex (Fig. 1, left; 600–610 nm).<sup>15b,17,23</sup> These facts suggest the auxiliary amino groups to be involved in the axial coordination to copper. Unfortunately, the  $\nu_{\text{as}}(\text{NH}_2)$  and  $\nu_{\text{s}}(\text{NH}_2)$  vibration modes of the amino group are concealed by the  $\nu(\text{OH})$  bands at 3500–3200  $\text{cm}^{-1}$  of the solvated methanol and water molecules. Two isomeric forms are considered for **L**<sup>1</sup> with respect to the *cis* or *trans* arrangement of two aminomethyl groups, but it is unclear if **1** contains one isomeric form or a mixture of two isomeric forms of **L**<sup>1</sup>. In spite of many efforts, we were unsuccessful in obtaining good crystals suitable to X-ray crystallographic study.

The condensation of **1** with two molecules of 2-formylpyridine afforded  $[\text{Cu}_2(\text{L}^2)](\text{ClO}_4)_2 \cdot 2\text{DMF}$  (**2**) in a good yield. We assumed this complex to have a di( $\mu$ -phenolato) dinuclear structure similar to that of **1**. However, the magnetic moment of **2** is common for magnetically diluted compounds (1.84  $\mu_{\text{B}}$  per Cu) and the moment was practically independent of temperature. Thus, the two copper centers of **2** must be considerably separated from each other. Eventually, X-ray structural study revealed that this complex has a unique structure with a large Cu...Cu separation as the consequence of the involvement of the 2-pyridylmethylimino residue in coordination. An ORTEP<sup>27</sup> view of **2** is shown in Fig. 4 together with the atom numbering scheme. Selected bond distances and angles are summarized in Table 2.

The essential part of **2** is represented by  $[\text{Cu}_2(\text{L}^2)]^{2+}$  with an inversion center: Two DMF molecules and two perchlorate ions are free from coordination and captured in the crystal lattice. The ligand **L**<sup>2</sup> assumes a unfolded, non-planar configuration with respect to the macrocyclic framework. The geometry about Cu is apparently planar with one imino nitrogen atom (N(1)) and one phenol oxygen atom (O(1)) from the macrocyclic framework and two nitrogen atoms (N(2) and N(3)) from the 2-pyridylmethylimino residue. The average Cu-to-donor

Table 2. Selected Bond Distances and Angles of  $[\text{Cu}_2(\text{L}^2)](\text{ClO}_4)_2 \cdot 2\text{DMF}$  (**2**)

Bond distances/Å			
Cu–O(1)	1.888(2)	Cu–N(1)	1.944(2)
Cu–N(2)	2.017(2)	Cu–N(3)	2.019(2)
Cu–N(4)* <sup>a</sup>	2.629(2)	Cu...Cu* <sup>a</sup>	4.434(1)
Bond angles/degree			
O(1)–Cu–N(1)	93.87(9)	O(1)–Cu–N(2)	168.88(9)
O(1)–Cu–N(3)	88.47(9)	N(1)–Cu–N(2)	96.32(10)
N(1)–Cu–N(3)	169.80(10)	N(2)–Cu–N(3)	80.73(10)

a) \*: Symmetry operation  $-x + 1, -y + 1, -z + 1$ .

bond distance is 1.967 Å. The imino nitrogen atom N(4) is located above Cu\* in a Cu\*...N(4) (Cu...N(4\*)) separation of 2.629(2) Å. Thus, the exact geometry about Cu can be regarded as an axially-elongated square-pyramid. The Cu...Cu\* interatomic separation is 4.434(1) Å. The ligand **L**<sup>2</sup> has the *trans* arrangement of two 2-pyridylmethylimino residues with respect to the macrocyclic framework, but we cannot rule out the possibility that **1** contains a mixture of *cis* and *trans* isomeric forms of **L**<sup>1</sup>.

The dinuclear structure of **2** is significantly stable, and we have failed in deriving a tetracopper assembly complex  $[\text{Cu}_4(\text{L}^2)(\text{A}-\text{A})_2]^{6+}$  from **2** using a bidentate ligand (A–A) such as 2,2'-bipyridine or 1,10-phenanthroline.

The condensation of **1** with two molecules of 3-[*N,N*-di(2-pyridylmethyl)aminomethyl]-5-methylsalicylaldehyde in the presence of  $\text{Cu}(\text{ClO}_4)_2 \cdot 6\text{H}_2\text{O}$  afforded the tetracopper assembly complex **3** in a tolerable yield. Positive ESI mass spectrometric studies in the presence of tetra(*n*-butyl)ammonium chloride indicated mass peaks centered at  $m/z = 1506$ ; this corresponds to  $\{\text{Cu}_4(\text{L}^3)\text{Cl}_3\}^+$ . The magnetic moment of **3** is 3.15  $\mu_{\text{B}}$  per molecule at 298 K and the moment decreased with lowering temperature to 2.74  $\mu_{\text{B}}$  at 2 K (Fig. 3). The  $\mu$  vs  $T$  curve can be explained in terms of one antiferromagnetically-interacting dinuclear  $\text{Cu}_2(\text{II},\text{II})$  unit and two magnetically-isolated mononuclear Cu(II) units,  $\mu^2 = \mu_{\text{CuCu}}^2 + 2\mu_{\text{Cu}}^2$ , using 1.93  $\mu_{\text{B}}$  for the mononuclear Cu(II) unit and the magnetic moment of **1** (trace **A** with no paramagnetic impurity) for the dinuclear  $\text{Cu}_2(\text{II},\text{II})$  unit. Thus, **3** can be formulated as  $\{\text{Cu}(\text{II})-\text{Cu}_2(\text{II},\text{II})-\text{Cu}(\text{II})\}$ . The electronic spectrum in DMF has absorption bands at 360 ( $\epsilon$ : 15200  $\text{dm}^3 \text{mol}^{-1} \text{cm}^{-1}$ ),  $\approx 380$  (shoulder), 420 (ca. 6000  $\text{dm}^3 \text{mol}^{-1} \text{cm}^{-1}$ ), and 665 nm (290  $\text{dm}^3 \text{mol}^{-1} \text{cm}^{-1}$ ). In comparison with the spectrum of **1**, the absorption bands at 360 and  $\approx 380$  nm may be associated with the dinuclear  $\text{Cu}_2(\text{II},\text{II})$  unit and the band at 420 nm with the mononuclear Cu(II) units. The absorption at 360 nm is ascribed to the  $\pi-\pi^*$  transition of the azomethine linkage.<sup>28,29</sup> The absorption at 665 nm is a superposition of the d–d bands of the four copper(II) ions.

**Redox Behavior of 3.** Our particular interest in this work is in the redox behavior of the tetracopper assembly complex **3**. The cyclic voltammogram of **3** in DMF has reversible or quasi-reversible couples at  $-0.77$ ,  $-0.85$ , and  $-1.29$  V vs  $\text{AgCl}/\text{Ag}$  (Fig. 5). Coulometric studies indicated three-electron transfer at  $-0.85$  V and four-electron transfer at  $-1.29$  V. We may conclude based on the wave heights that the couple at  $-0.77$  V involves two-electron transfer and the couple at

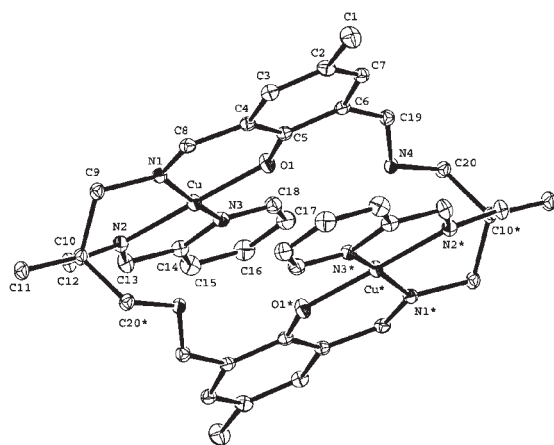


Fig. 4. An ORTEP view of  $[\text{Cu}_2(\text{L}^2)](\text{ClO}_4)_2 \cdot 2\text{DMF}$  (**2**) with the atom numbering scheme.



−0.85 V involves one-electron transfer. The three-electron reduced solution has a broad absorption band around 1000 nm characteristic of the intervalence transition of the mixed-spin  $\text{Cu}_2(\text{I,II})$  complex<sup>15,16</sup> in addition to a d–d band at  $\approx 600$  nm (see Fig. 7).

The three-electron reduced solution at room temperature shows a unresolved EPR signal around 3000 G with a band width of ca. 450 G (Fig. 6, left). This resembles the EPR of the mixed-spin  $\text{Cu}_2(\text{I,II})$  species of the parent complex (Fig. 1, left),<sup>15,16</sup> despite the lack of a seven-line hyperfine structure. The absence of hyperfine splitting is probably due to slow tangling of the tetracopper assembly in solution. The frozen solution of the reduced solution at liquid nitrogen temperature, on the other hand, shows an axial pattern of EPR with  $g_{\parallel} = 2.22$  and  $g_{\perp} = 2.03$ , and a four-line hyperfine structure superimposed on the  $g_{\parallel}$  component ( $A_{\parallel} = 190 \times 10^{-4} \text{ cm}^{-1}$ ) (Fig. 6, right). Evidently, the valence of the  $\text{Cu}_2(\text{I,II})$  species is localized in the frozen solution at liquid nitrogen temperature. From these visible spectroscopic and EPR results, the three-electron reduced species has the oxidation state of  $\{\text{Cu}(\text{I})\text{--Cu}_2(\text{I,II})\text{--Cu}(\text{I})\}$ , and the redox couple at −1.29 V is

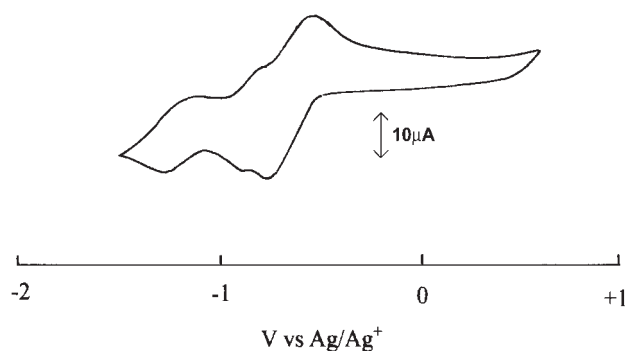
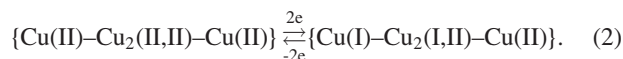


Fig. 5. Cyclic voltammogram of  $[\text{Cu}_4(\text{L}^3)](\text{ClO}_4)_4 \cdot 3\text{H}_2\text{O}$  (**3**) in DMF. Conditions: GC working electrode, Pt wire counter electrode,  $\text{AgCl}/\text{Ag}$  reference electrode, TBAP (0.1 M) supporting electrolyte, scan rate  $100 \text{ mV s}^{-1}$ .

concerned with the  $\{\text{Cu}(\text{I})\text{--Cu}_2(\text{I,II})\text{--Cu}(\text{I})\}/\{\text{Cu}(\text{I})\text{--Cu}_2(\text{I,I})\text{--Cu}(\text{I})\}$  process. The four-electron reduced solution assumes a yellow color in accord with its fully reduced oxidation state,  $\{\text{Cu}(\text{I})\text{--Cu}_2(\text{I,I})\text{--Cu}(\text{I})\}$ .

The two-electron process at −0.77 V is supposed to be concerned with the redox of two mononuclear  $\text{Cu}(\text{II})$  units. In order to examine the redox process in detail, **3** was reduced by one electron or two electrons at −0.77 V and the reduced solutions were subjected to spectroscopic studies. The absorption spectra of the one-electron reduced solution (**3-e**) and the two-electron reduced solution (**3-2e**) are given in Fig. 7, together with the spectra of **3** and its three-electron reduced solution (**3-3e**). The near UV spectra of **3–3-3e** (Insert) vary complicatedly on the stepwise reduction. We focus our attention on the spectra in the visible and near IR region.

The visible spectrum of **3-e** is similar to the spectrum of **3** except that the d–d band maximum slightly shifts to a shorter wavelength and its intensity becomes weaker. The spectral change is understood by the reduction of one mononuclear  $\text{Cu}(\text{II})$  unit to afford a  $\{\text{Cu}(\text{I})\text{--Cu}_2(\text{II,II})\text{--Cu}(\text{II})\}$  species. A drastic spectral change occurs on going from **3-e** to **3-2e**, and the spectrum of **3-2e** has a broad absorption around 1000 nm characteristic of the intervalence transition of mixed-valence  $\text{Cu}_2(\text{I,II})$  complexes.<sup>14,15</sup> This fact means that an intramolecular electron transfer occurs from one  $\text{Cu}(\text{I})$  unit to the dinuclear  $\text{Cu}_2(\text{II,II})$  unit when two  $\text{Cu}(\text{II})$  units are reduced to  $\text{Cu}(\text{I})$ :  $\{\text{Cu}(\text{II})\text{--Cu}_2(\text{II,II})\text{--Cu}(\text{II})\}/\{\text{Cu}(\text{I})\text{--Cu}_2(\text{II,II})\text{--Cu}(\text{I})\} \rightarrow \{\text{Cu}(\text{I})\text{--Cu}_2(\text{I,II})\text{--Cu}(\text{II})\}$ . The good reversibility of the CV indicates that the intramolecular electron transfer is fast enough to be completed within the scan rate of CV measurement ( $100 \text{ mV s}^{-1}$ ). It is also likely that the intramolecular electron transfer occurs reversibly on reduction and re-oxidation processes:



The spectrum of **3-3e** resembles the spectrum of **3-2e** except for a decrease in intensity of the d–d band at  $\approx 620$  nm. There-

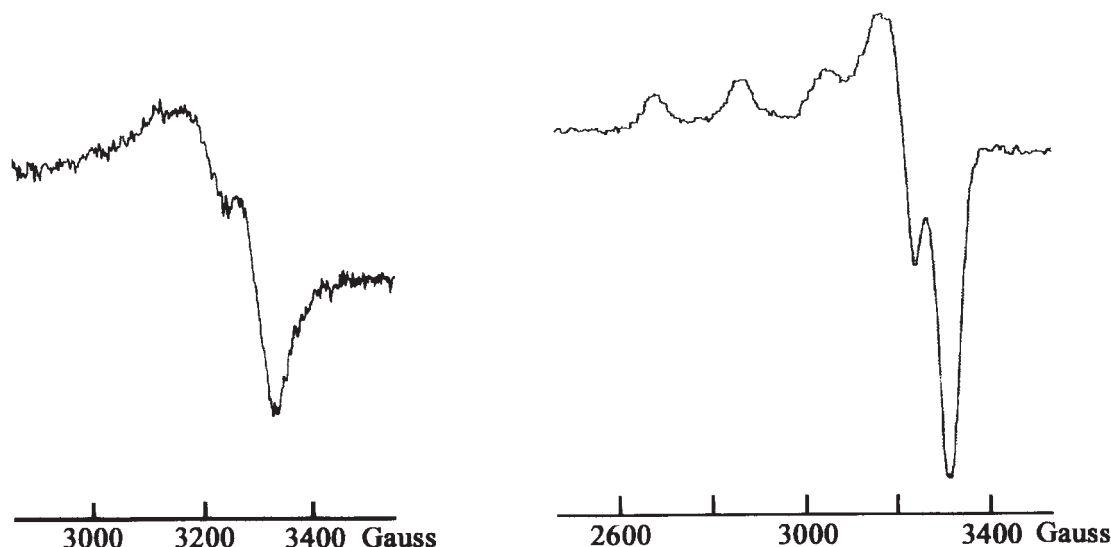


Fig. 6. EPR spectra of three-electron reduced complex of **3** in DMF: (left) at room temperature, (right) at liquid nitrogen temperature.

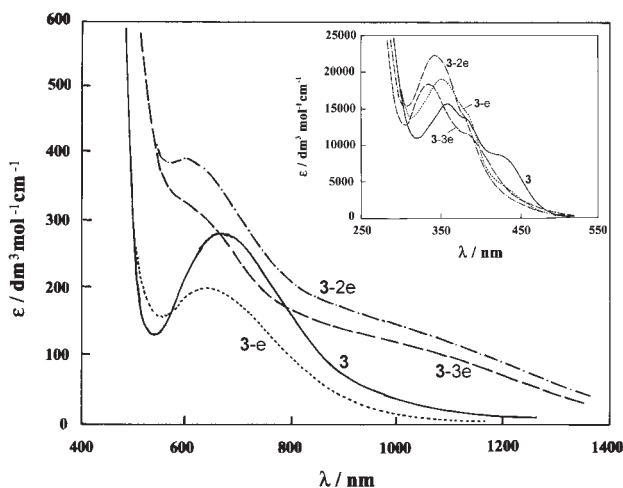


Fig. 7. Visible and near IR spectra of **3**, one-electron reduced solution (**3-e**), two-electron reduced solution (**3-2e**), and three-electron reduced solution (**3-3e**) in DMF. The spectra in the near ultraviolet region are given in the insert.

fore, the redox couple at  $-0.85$  V is associated with the process:  $\{\text{Cu(I)}\text{--Cu}_2(\text{I,II})\text{--Cu(II)}\} / \{\text{Cu(I)}\text{--Cu}_2(\text{I,I})\text{--Cu(I)}\}$ .

The present study using the tetracopper assemble complex **3** clearly demonstrates that an intramolecular electron transfer occurs from one reduced Cu(I) unit to the dinuclear  $\text{Cu}_2(\text{II,II})$  center when two Cu(II) units are reduced to Cu(I). It must be emphasized that such an electron transfer does not occur when one of the Cu(II) units is reduced. Thus, **3** illustrates the significance of the tetracopper constellation in multicopper oxidases: reduced type 1 copper transfers an electron, in conjunction with reduced type 2 copper, to type 3 copper. The origin for the intramolecular electron transfer in the tetracopper assembly complex, and in multicopper oxidases as well, remains to be examined further.

### Conclusion

A di( $\mu$ -phenolato) dinuclear copper(II) complex,  $[\text{Cu}_2(\text{L}^1)](\text{ClO}_4)_2 \cdot \text{CH}_3\text{OH} \cdot 2\text{H}_2\text{O}$  (**1**), with the macrocyclic ligand  $\text{L}^1$  derived from the [2:2] cyclic condensation between 2,6-diformyl-4-methylphenol and 1,1,1-tri(aminomethyl)ethane, was adopted as type 3 copper site for modeling multicopper oxidase. The condensation of **1** through two auxiliary amino groups on the macrocyclic framework of  $\text{L}^1$  with two molecules of 2-formylpyridine afforded  $[\text{Cu}_2(\text{L}^2)](\text{ClO}_4)_2 \cdot 2\text{DMF}$  (**2**). This has a dinuclear structure different from di( $\mu$ -phenolato)dinuclear copper(II), owing to the involvement of the auxiliary 2-pyridylmethylimino residues in coordination. This complex cannot be converted into tetracopper assembly complexes. The condensation of **1** with two molecules of 3-[*N,N*-di(2-pyridylmethyl)aminomethyl]-5-methylsalicylaldehyde, in the presence of  $\text{Cu}(\text{ClO}_4)_2 \cdot 6\text{H}_2\text{O}$ , afforded the tetracopper assembly complex,  $[\text{Cu}_4(\text{L}^3)](\text{ClO}_4)_4 \cdot 3\text{H}_2\text{O}$  (**3**) which is comprised of a macrocyclic dinuclear  $\text{Cu}_2(\text{II,II})$  unit and two auxiliary mononuclear Cu(II) units,  $\{\text{Cu(II)}\text{--Cu}_2(\text{II,II})\text{--Cu(II)}\}$ . The cyclic voltammogram of **3** exhibited a two-electron redox process at  $-0.77$  V (vs  $\text{Ag}/\text{Ag}^+$ ) followed by two one-electron redox processes at  $-0.85$  and  $-1.29$  V. Coulometric studies

combined with spectroscopic studies demonstrated that the redox process at  $-0.77$  V involves the reduction of the two mononuclear Cu(II) units followed by a fast intramolecular electron transfer from one of the reduced Cu(I) units to the dinuclear  $\text{Cu}_2(\text{II,II})$  unit:  $\{\text{Cu(II)}\text{--Cu}_2(\text{II,II})\text{--Cu(II)}\} / \{\text{Cu(I)}\text{--Cu}_2(\text{II,II})\text{--Cu(I)}\} \rightarrow \{\text{Cu(I)}\text{--Cu}_2(\text{I,II})\text{--Cu(II)}\}$ . The resulting  $\{\text{Cu(I)}\text{--Cu}_2(\text{I,II})\text{--Cu(II)}\}$  species is further reduced to  $\{\text{Cu(I)}\text{--Cu}_2(\text{II,I})\text{--Cu(I)}\}$  at  $-0.85$  V and to  $\{\text{Cu(I)}\text{--Cu}_2(\text{I,I})\text{--Cu(I)}\}$  at  $-1.29$  V. The intramolecular electron transfer observed for **3** is relevant to multicopper oxidase: reduced type 1 copper transfers an electron, in conjunction with reduced type 2 copper, to type 3 copper.

We thank Dr. Hisashi Shimakoshi and Prof. Yoshio Hisaeda of Kyushu University for ESI mass measurements. This work was supported by a Grant-in-Aid for Scientific Research (No. 07454178) from the Ministry of Education, Culture, Sports, Science and Technology.

### References

- 1 E. I. Solomon, M. J. Baldwin, M. D. Lowery, *Chem. Rev.* **1992**, 92, 521.
- 2 E. I. Solomon, M. D. Lowery, *Science* **1993**, 259, 1575.
- 3 J. A. Fee, *Struct. Bonding (Berlin)* **1975**, 23, 1.
- 4 K. G. Strothkamp, C. R. Dawson, *Biochemistry* **1974**, 13, 434.
- 5 A. Messerschmidt, A. Rossi, R. Ladenstein, R. Huber, M. Bolognesi, G. Gatti, A. Marchesini, R. Petruzzelli, A. Finazzo-Ago, *J. Mol. Biol.* **1989**, 206, 513.
- 6 I. Zaitsev, V. Zaitsev, G. Card, K. Moshkov, B. Bax, A. Ralph, P. Lindley, *Biol. Inorg. Chem.* **1996**, 1, 15.
- 7 J. L. Cole, G. O. Tan, E. K. Yang, K. O. Hodgson, E. I. Solomon, *J. Am. Chem. Soc.* **1990**, 112, 2243.
- 8 K. D. Karlin, Q.-F. Gan, A. Farooq, S. Liu, J. Zubieta, *Inorg. Chem.* **1990**, 29, 2549.
- 9 a) H. Adams, N. A. Bailey, M. J. S. Dwyer, D. E. Fenton, P. C. Hellier, P. D. Hampstead, *J. Chem. Soc., Chem. Commun.* **1991**, 1297. b) H. Adams, N. A. Bailey, M. J. S. Dwyer, D. E. Fenton, P. C. Hellier, P. D. Hampstead, J.-M. Latour, *J. Chem. Soc., Dalton Trans.* **1993**, 1207.
- 10 P. Hubberstey, C. E. Russell, *J. Chem. Soc., Chem. Commun.* **1995**, 959.
- 11 B. G. Malmstrom, *Annu. Rev. Biochem.* **1982**, 51, 21.
- 12 K. Motoda, M. Aiba, C. Kokubo, N. Matsumoto, H. Ōkawa, *Chem. Lett.* **1995**, 1065.
- 13 S. Yamanaka, H. Ōkawa, K. Motoda, M. Yonemura, D. E. Fenton, M. Ebadi, A. B. P. Lever, *Inorg. Chem.* **1999**, 38, 1825.
- 14 G. A. Melson, *Coordination Chemistry of Macrocyclic Compounds*, Plenum Press, New York and London, **1979**.
- 15 a) R. R. Gagné, C. A. Koval, T. J. Smith, *J. Am. Chem. Soc.* **1977**, 99, 8368. b) R. R. Gagné, C. A. Koval, T. J. Smith, M. C. Cimolino, *J. Am. Chem. Soc.* **1979**, 101, 4571.
- 16 R. C. Long, D. N. Hendrickson, *J. Am. Chem. Soc.* **1983**, 105, 1513.
- 17 S. K. Mandal, K. Nag, *J. Chem. Soc., Dalton Trans.* **1983**, 2429.
- 18 D. A. Denton, H. Suschitzky, *J. Chem. Soc.* **1963**, 4741.
- 19 E. B. Fleischer, A. E. Gebala, A. Levey, P. A. Tasker, *J. Org. Chem.* **1971**, 36, 3042.
- 20 R. J. Geue, G. H. Searle, *Aust. J. Chem.* **1983**, 36, 927.

- 21 S. Uozumi, H. Furutachi, M. Ohba, H. Ōkawa, D. E. Fenton, K. Shindo, S. Murata, D. J. Kitko, *Inorg. Chem.* **1998**, 37, 6281.
- 22 *teXsan: Crystal Structure Analysis Package*, Molecular Structure Corporation, Houston, TX, **1985** and **1999**.
- 23 N. H. Pilkington, R. Robson, *Aust. J. Chem.* **1970**, 23, 2225.
- 24 S. L. Lambert, D. N. Hendrickson, *Inorg. Chem.* **1979**, 18, 2683.
- 25 B. Bleaney, K. D. Bowers, *Proc. R. Soc. London, Ser. A* **1952**, 214, 451.
- 26 H. Ōkawa, S. Kida, *Bull. Chem. Soc. Jpn.* **1972**, 45, 1759.
- 27 C. K. Johnson, *Report 3794*, Oak Ridge National Laboratory, Oak Ridge, TN, **1965**.
- 28 B. Bosnich, *J. Am. Chem. Soc.* **1968**, 90, 627.
- 29 R. S. Downing, F. L. Urbach, *J. Am. Chem. Soc.* **1969**, 91, 5977.